Materials Transactions, JIM, Vol. 38, No. 7 (1997), pp. 577 to 582

Thermal and Magnetic Properties of $Fe_{56}Co_7Ni_7Zr_{10-x}Nb_xB_{20}$ Amorphous Alloys with Wide Supercooled Liquid Range

Akihisa Inoue*, Hisato Koshiba*†, Tao Zhang*
and Akihiro Makino**

*Institute for Materials Research, Tohoku University, Sendai 980-77, Japan
**Alps Electric Co. Ltd., Nagaoka 940, Japan

Amorphous alloys with a wide supercooled liquid region of 45 to 85 K were found to be formed in $Fe_{56}Co_7Ni_7Zr_{10-x}Nb_xB_{20}$ (x=0 to 10 at%) alloys by melt spinning. The glass transition temperature (T_g) and the crystallization temperature (T_x) increase by the dissolution of 2 to 4%Nb. The degree of increase is larger for T_x than T_g, leading to the maximum $\Delta T_x(=T_x-T_g)$ of 85 K for the 2%Nb alloy. The ΔT_x value is about 20 K larger than the largest value for the newly developed Fe-(Al, Ga)-(P, C, B, Si) amorphous alloys. The crystallization occurs through a single stage, amorphous→α-Fe+γ-Fe+Fe_2Zr+$Fe_{76}Nb_6B_{18}$, for the alloys containing less than about 6%Nb and through two stages, amorphous→amorphous+γ-Fe→γ-Fe+$Co_3Nb_2B_5$+Ni_8Nb, for the alloys containing more than 8%Nb. The change in the crystallization process for the Nb-rich alloys probably reflects the disappearance of Fe_2(Nb, Zr) precipitates because of the weaker bonding of Fe-Nb pair as compared with Fe-Zr one. As the Nb content increases, the saturation magnetization (I_s) and permeability (μ_e) of the annealed alloys decrease while the coercive force (H_c) remains almost unchanged. The good soft magnetic properties are obtained for the alloys containing less than 2%Nb subjected to annealing for 300 s at 800 K and the I_s, H_c and μ_e at 1 kHz are 0.96 T, 2.0 A/m and 19100, respectively, for the 0%Nb alloy and 0.75 T, 1.1 A/m and 25000, respectively, for the 2%Nb alloy. The success of synthesizing the new amorphous alloys with a wide supercooled liquid region more than 80 K and with good soft magnetic properties is promising for future development as soft magnetic bulk amorphous alloys.

(Received February 5, 1997)

Keywords: *soft magnetic amorphous alloy, wide supercooled liquid region, glass transition, iron-based alloy system, melt spinning, soft magnetic property, single stage crystallization process*

I. Introduction

Since the findings of new amorphous alloys with large glass-forming ability in Mg-Ln-TM[1][2], Ln-Al-TM[3][4] and Zr-Al-TM[5][6] (Ln=lanthanide metal, TM=transition metal) systems from 1988 to 1991, significant attention has been paid to the new multicomponent amorphous systems in which bulk amorphous alloys can be prepared by a copper mold casting process. The bulk amorphous alloys had been limited to the non-ferromagnetic Mg-[7][8], Ln-[9][10] and Zr-[11]-[13] base systems. Subsequently, a search of bulk amorphous alloys with ferromagnetism at room temperature was carried out in the framework of the three empirical rules for the achievement of large glass-forming ability[14]-[19]. As a result, ferromagnetic bulk amorphous alloys have been found in the Fe-(Al, Ga)-(P, B, C, Si, Ge)[20][21] and (Nd, Pr)-Fe-(Al, Ga)[22]-[25] systems. The former Fe-based bulk amorphous alloys are obtained in the diameter range up to 2 mm and exhibit good soft magnetic properties of 1.1 to 1.3 T for saturation magnetization (I_s), 2 to 5 A/m for coercive force (H_c) and 5000 to 7000 for permeability (μ_e) at 1 kHz. On the other hand, the latter Nd- and Pr-based bulk amorphous alloys are prepared in the diameter range up to 12 mm and have rather good hard magnetic properties, i.e., intrinsic coercive force ($_iH_c$) of 250 to 600 kA/m, remanence (B_r) of 0.1 to 0.2 T and maximum energy product $(BH)_{max}$ of 10 to 20 kJ/m^3. Considering that the soft magnetic properties of the Fe-based bulk amorphous alloys are comparable to those[26][27] for the commercial Fe-Si-B sheet amorphous alloys, the appearance of Fe-based amorphous alloys with larger glass-forming ability is expected to cause a further extension of application field of soft magnetic amorphous alloys. More recently, based on the three empirical rules[15]-[19] for the achievement of large glass-forming ability, we have searched a new Fe-based amorphous alloy with a wider supercooled liquid region, namely, a larger glass-forming ability, and succeeded[28] in finding new multicomponent Fe-based amorphous alloys with the largest ΔT_x value of 73 K in $(Fe, Co, Ni)_{70}Zr_{10}B_{20}$ system. Subsequently, we have examined the effect of the partial replacement of Zr by Nb corresponding to the further increase in the degree of the satisfaction of the three empirical rules and noticed that the replacement by 2 at%Nb causes a significant increase in ΔT_x to 85 K. This paper is intended to present the compositional dependence of T_g, T_x, ΔT_x, crystallization behavior and magnetic properties for $Fe_{56}Co_7Ni_7Zr_{10-x}Nb_xB_{20}$ amorphous alloys and to investigate the reason for the increase in the thermal stability of the supercooled liquid region for the 2%Nb-con-

† Permanent address: Alps Electric Co. Ltd., Nagaoka 940, Japan.

taining alloy.

II. Experimental Procedure

Multicomponent alloys with composition $Fe_{56}Co_7Ni_7Zr_{10-x}Nb_xB_{20}$ were examined in the present study because the $Fe_{56}Co_7Ni_7Zr_{10}B_{20}$ amorphous alloy had the widest supercooled liquid region before crystallization. Their master ingots were prepared by arc melting the mixture of pure Fe, Co, Ni, Zr and Nb metals and pure B crystal in an argon atmosphere. The alloy compositions represent the nominal atomic percentage of the mixture. Rapidly solidified ribbons with a cross section of $0.015 \times 1.0\ mm^2$ were prepared by melt spinning the master ingots in an argon atmosphere. The amorphous structure was confirmed by X-ray diffractometry and transmission electron microscopy. Thermal stability associated with glass transition, supercooled liquid region and crystallization was examined by differential scanning calorimetry (DSC) at a heating rate of 0.67 K/s. The saturation magnetization and residual magnetization at room temperature were measured in a maximum applied field of 1260 kA/m with a vibrating sample magnetometer (VSM). The coercive force was measured with a B-H loop tracer. Permeability was evaluated at 1 kHz with an impedance analyzer.

III. Results

Figure 1 shows the X-ray diffraction patterns of the melt-spun $Fe_{56}Co_7Ni_7Zr_{10-x}Nb_xB_{20}$ (x=0, 2, 4, 6, 8 and 10 at%) alloys. Only a broad peak is seen at a wave vector ($K_p=4\pi \sin\theta/\lambda$) of about $30.2\ nm^{-1}$ ($2\theta \cong 44$ deg) and no diffraction peak corresponding to a crystalline phase is seen for all the alloys. The X-ray diffraction data indicate clearly that these melt-spun alloys are composed of an amorphous phase. Figure 2 shows the DSC curves of the melt-spun $Fe_{56}Co_7Ni_7Zr_{10-x}Nb_xB_{20}$ (x=0, 2, 4, 6, 8 and 10 at%) amorphous alloys. It is to be noticed that a glass transition, followed by a wide supercooled liquid region is observed distinctly in the temperature range before crystallization for all the alloys. However, the crystallization behavior changes from a single stage to two stages for the alloy composition around 7 at%Nb. Based on these DSC curves, the glass transition temperature (T_g), the onset temperature of crystallization (T_x) and the temperature interval of supercooled liquid region ($\Delta T_x = T_x - T_g$) for the Fe-Co-Ni-Zr-Nb-B amorphous alloys were plotted as a function of Nb content in Fig. 3. The T_g and T_x are 814 and 887 K, respectively, for the 0%Nb alloy. They increase by the dissolution of Nb to show maximum values of 828 and 912 K, respectively, for the alloys containing 2 to 4 at%Nb and then decrease significantly with a further increase in Nb content. The degree of increase in T_x is larger than that in T_g, leading to the increase in ΔT_x from 73 K for the 0%Nb alloy to 85 K for the 2%Nb alloy. Here, it is important to point out that the $Fe_{56}Co_7Ni_7Nb_{10}B_{20}$ amorphous alloy also exhibits the glass transition and a wide supercooled liquid

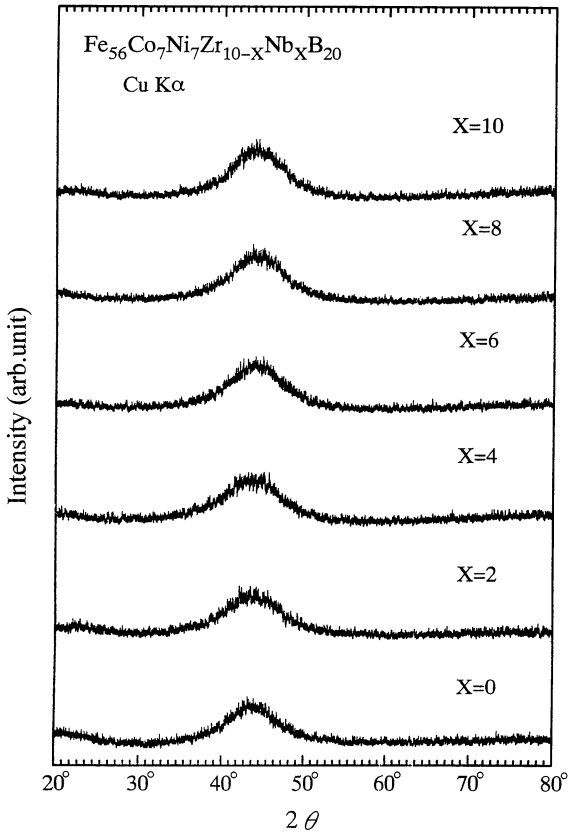

Fig. 1 X-ray diffraction patterns of the melt-spun $Fe_{56}Co_7Ni_7Zr_{10-x}Nb_xB_{20}$ (x=0, 2, 4, 6, 8 and 10 at%) alloys.

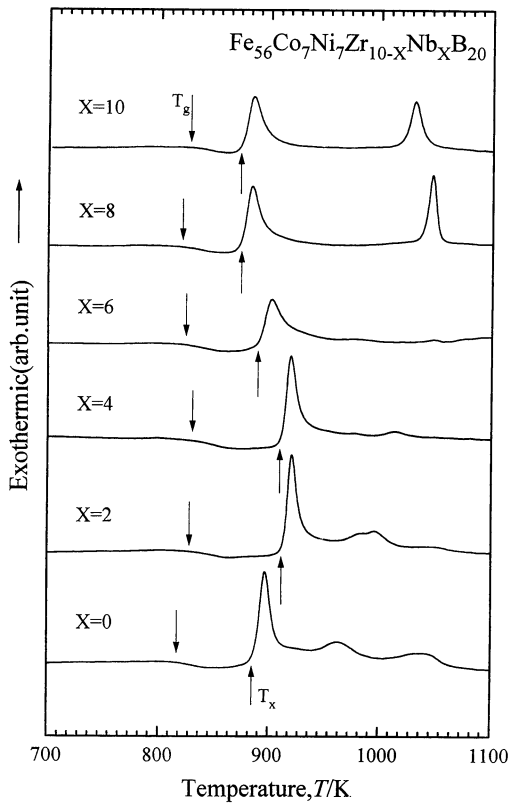

Fig. 2 Differential scanning calorimetric curves of the amorphous $Fe_{56}Co_7Ni_7Zr_{10-x}Nb_xB_{20}$ alloys.

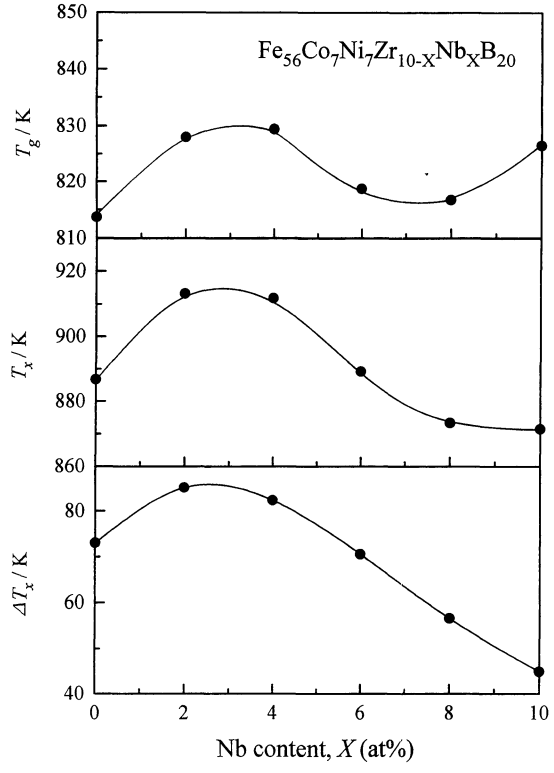

Fig. 3 Changes in the glass transition temperature (T_g), onset temperature of crystallization (T_x) and temperature interval of supercooled liquid region ($\Delta T_x = T_x - T_g$) as a function of Nb content for the amorphous $Fe_{56}Co_7Ni_7Zr_{10-x}Nb_xB_{20}$ alloys.

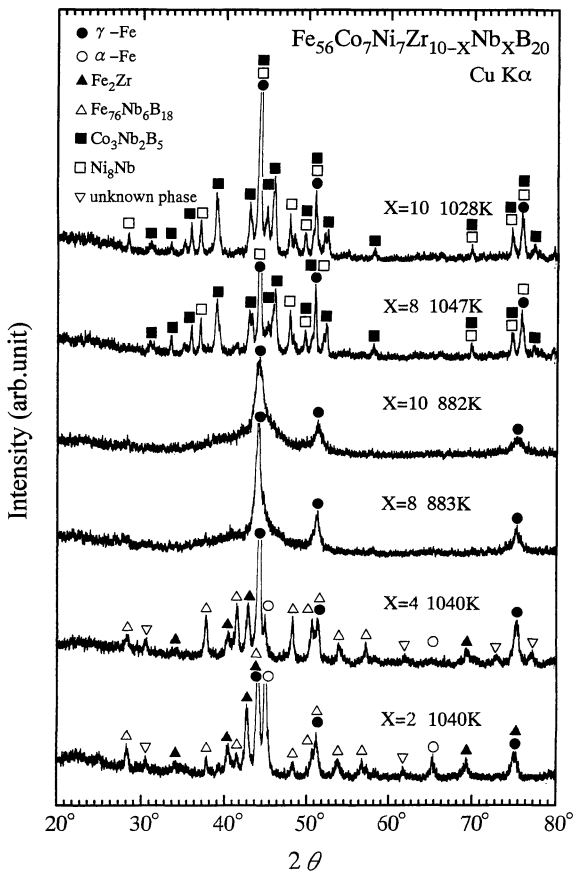

Fig. 4 X-ray diffraction patterns of the amorphous $Fe_{56}Co_7Ni_7Zr_{10-x}Nb_xB_{20}$ (x=2, 4, 8 and 10 at%) alloys annealed for 600 s at the temperatures above the exothermic peaks.

region.

With the aim of clarifying the reason for the change in the crystallization behavior around 7 at%Nb, the X-ray diffraction patterns of the $Fe_{56}Co_7Ni_7Zr_{10-x}Nb_x$ (x=2, 4, 8 and 10 at%) alloys heated for 600 s at the temperatures above the exothermic peaks were examined. The X-ray diffraction patterns (Fig. 4) were identified to consist of α-Fe, γ-Fe, Fe_2Zr and $Fe_{76}Nb_6B_{18}$ phases for the 2 and 4 at%Nb alloys with a single exothermic peak, a γ-Fe phase for the 8 and 10 at%Nb alloys heated to 883 K corresponding to the temperature just above the first exothermic peak and γ-Fe, $Co_3Nb_2B_5$ and Ni_8Nb phases for the 8 and 10 at%Nb alloys heated to 1028 to 1047 K just above the second exothermic peak. From the identification, it is concluded that the crystallization occurs with a single stage (amorphous→α-Fe+γ-Fe+Fe_2Zr+$Fe_{76}Nb_6B_{18}$) for the alloys containing less than about 6 at%Nb, and with two stages (amorphous→γ-Fe+amorphous→γ-Fe+$Co_3Nb_2B_5$+Ni_8Nb) for the alloys containing more than 8 at%Nb. It is to be noticed that the two-stage crystallization occurs when the Fe_2(Nb, Zr) phase is not formed. It has been reported that the predicted negative heat of mixing for an equiatomic alloy is 37 kJ/mol for Fe-Zr, 38 kJ/mol for Fe-B, 102 kJ/mol for Zr-B, 23 kJ/mol for Fe-Nb, 79 kJ/mol for Nb-B, 37 kJ/mol for Co-Nb and 45 kJ/mol for the Ni-Nb systems[29]. These values suggest that the bonding force for the Fe-Nb pair is considerably weaker as compared with any other atomic pairs. The weakest bonding force of Fe-Nb pair is thought to allow the generation of isolated Fe-Fe bonding pairs, leading to the change in the crystallization process from a single stage to two stages due to the additional precipitation of the γ-Fe phase in the alloys containing more than 8 at%Nb. This is possibly the first evidence for the appearance of a wide supercooled liquid region exceeding 45 K in amorphous alloys where the crystallization occurs with two distinct stages where temperature interval is as large as about 150 K.

Figures 5 and 6 show hysteresis I-H loops of $Fe_{56}Co_7Ni_7Zr_{10-x}Nb_xB_{20}$ amorphous alloys in as-quenched and annealed (300 s, 800 K) states, respectively. It is seen that the replacement of Zr by Nb for the as-quenched samples causes a decrease in I_s from 0.92 T at 0 at%Nb to 0.54 T at 10 at%Nb through 0.74 T at 2 at%Nb and an increase in H_c from 5.2 A/m at 0 at%Nb to 41.3 A/m at 10%Nb through 5.5 A/m at 2%Nb. On the other hand, the annealed samples exhibit a monotonous decrease in I_s from 0.96 T at 0%Nb to 0.61 T at 10%Nb as well as a nearly constant low H_c of about 1.1 A/m in the whole Nb content range. It is thus to be noticed that the H_c decreases significantly by the optimal annealing treatment. Figures 5 and 6 also show that the annealing causes a marked increase in the squareness ratio defined by the ratio of residual magnetization (I_r) to I_s for the alloys con-

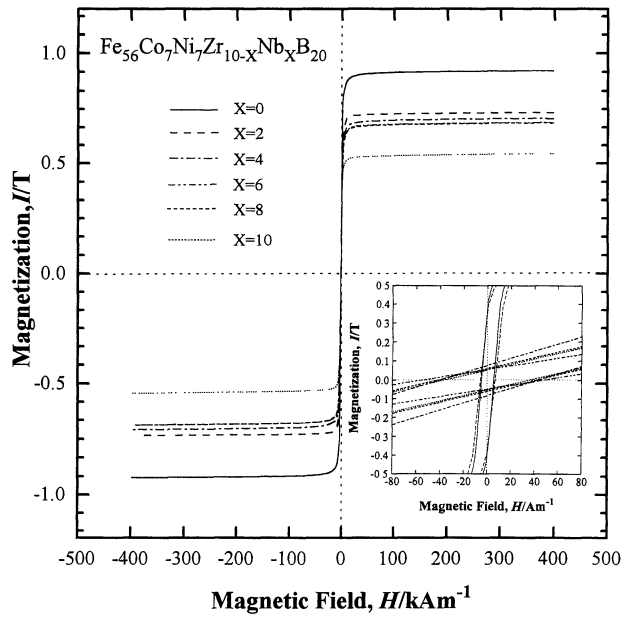

Fig. 5 Hysteresis *I-H* loops of the amorphous $Fe_{56}Co_7Ni_7Zr_{10-x}Nb_xB_{20}$ alloys in the as-quenched state.

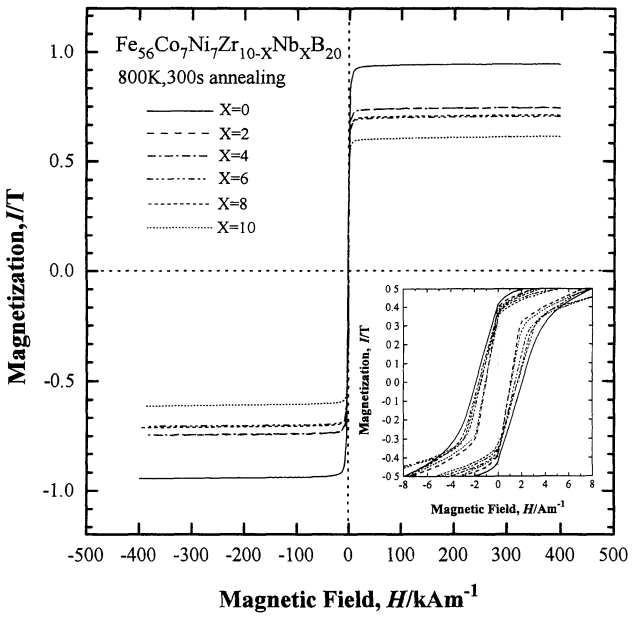

Fig. 6 Hysteresis *I-H* loops of the amorphous $Fe_{56}Co_7Ni_7Zr_{10-x}Nb_xB_{20}$ alloys in the state annealed for 300 s at 800 K.

taining 4 to 10%Nb. Although the total amount of Fe and Co elements remains constant, it is seen that the I_s for the annealed samples shows a decrease of 0.21 T only by the dissolution of 2 at%Nb. The significant decrease probably reflects the lowering of Curie temperature with increasing Nb content. Figure 7 shows changes in effective permeability (μ_e) at 1 kHz and saturated magnetostriction (λ_s) as a function of Nb content for the $Fe_{56}Co_7Ni_7Zr_{10-x}Nb_xB_{20}$ amorphous alloys in as-quenched and annealed states, together with those of I_s and H_c. The μ_e increases significantly by annealing and reaches 19100 at 0 at%Nb and 25000 at 2 at%Nb. With a further increase in Nb content, the μ_e decreases gradually to 14800 at 10 at%Nb. The compositional dependence is analogous to that for I_s. It is also confirmed that the H_c of the alloys containing more than 4 at%Nb decreases signifiicantly from about 45 A/m to about 1 A/m by annealing. The λ_s keeps a relatively low level of about 10×10^{-6} in the whole Nb content range and remains almost unchanged in the as-quenched and annealed states. The λ_s value is considerably lower than that (about 30×10^{-6})[26][27] for conventional Fe-Si-B amorphous ribbon alloys. The lower λ_s is thought to be one of the reasons for the simultaneous achievement of lower H_c and higher μ_e as compared with Fe-Si-B amorphous alloys. Although the reason for the significant change in H_c in the vicinity of 3 at%Nb for the as-quenched samples with nearly the same λ_s values remains unknown, it may be related to the decrease in the glass-forming ability resulting from the decrease in ΔT_x. From the compositional dependence of the thermal stability of the supercooled liquid and the magnetic properties, it is concluded that the $Fe_{56}Co_7Ni_7Zr_{10-x}Nb_xB_{20}$ amorphous alloys containing 0 to 2 at%Nb have the combination of large glass-forming ability and good soft magnetic properties.

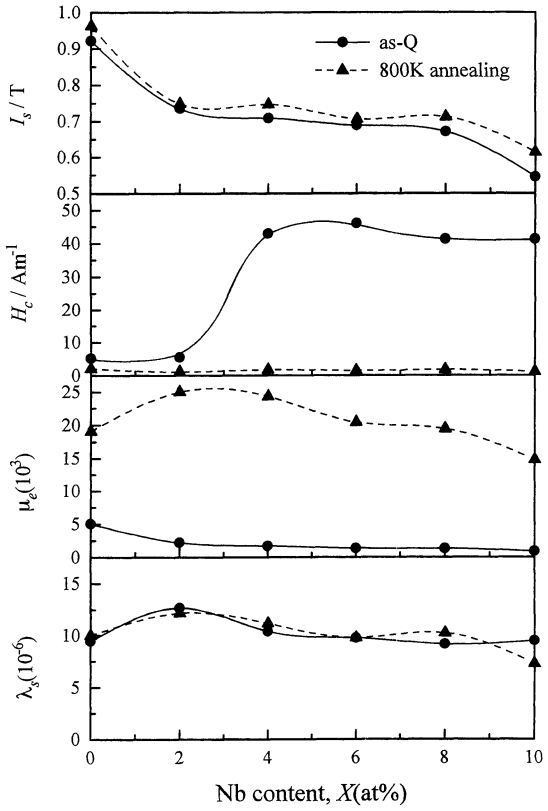

Fig. 7 Changes in saturation magnetization (I_s), coercive force (H_c), permeability at 1 kHz (μ_e) and saturated magnetostriction (λ_s) as a function of Nb content for the amorphous $Fe_{56}Co_7Ni_7Zr_{10-x}Nb_xB_{20}$ alloys in the as-quenched and annealed (300 s, 800 K) states.

IV. Discussion

It was shown in Figs. 2 and 3 that the replacement of Zr by 2 to 4 at%Nb causes the significant extension of the supercooled liquid region defined by the difference in T_g and T_x through the increase in T_x exceeding the degree of the increase in T_g as a function of Nb content. It is to be noticed that the largest ΔT_x value of 86 K for the 2 at% Nb alloy is larger by about 20 K than the largest value (66 K)[30] for Fe-based amorphous alloys reported up to date. The significant increase in ΔT_x allows us to expect that the new Fe-Co-Ni-Zr-Nb-B alloy has a large glass-forming ability which enables the production of bulk amorphous alloys with diameters above several milimeters by the copper mold casting process. Consequently, it is important to discuss the reason for the significant extension of the supercooled liquid region before crystallization by the dissolution of 2 to 4 at%Nb. It has previously been pointed out that the appearance of the wide supercooled liquid region of 73 K[28] for the Fe-Co-Ni-Zr-B alloys without Nb is due to the satisfaction of the three empirical rules for the achievement of large glass-forming ability, namely, (1) the multicomponent system consisting of more than three constituent elements, (2) the significantly different atomic size ratios above about 12% among the three main constituent elements, as is evidenced from the change Zr $\gg$ Fe $>$ Co $=$ Ni $\gg$ B[31], and (3) the large negative heats of mixing among the main constituent elements, as is evidenced from the negative enthalpies of mixing of 37 to 72 kJ/mol for Fe-Zr, Co-Zr and Ni-Zr pairs, 33 to 38 kJ/mol for Fe-B, Co-B and Ni-B pairs and 102 kJ/mol for Zr-B pair[29]. The addition of an appropriate amount (2 to 4 at%) of Nb is expected to cause an enhancement of the degree of the satisfaction of the three empirical rules. That is, the atomic size changes more continuously in the order of Zr $\gg$ Nb $\gg$ Fe $>$ Co $=$ Ni $\gg$ B[31] and additional atomic pairs of Fe-Nb, Co-Nb, Ni-Nb and Nb-B with large negative heats of mixing generate for the Nb-containing alloys. However, the heat of mixing is 23 to 45 kJ/mol for the Fe-Nb, Co-Nb and Ni-Nb pairs and 79 kJ/mol for the Nb-B pair[29], being considerably smaller than those for the corresponding Fe-Zr, Co-Zr, Ni-Zr and Zr-B pairs. The weaker bonding nature of the main Fe-Nb atomic pair seems to result in the decrease in ΔT_x for the alloys containing more than 8 at%Nb owing to the primary precipitation of the γ-Fe phase resulting in a change from a single-stage crystallization process to a two-stage process. This change indicates clearly the importance of an attractive bonding nature among the constituent elements for the achievement of a wide supercooled liquid region before crystallization in addition to the significantly different atomic size ratios.

V. Summary

With the aim of searching a new amorphous alloy with a wide supercooled liquid region before crystallization and good soft magnetic properties, the compositional dependence of T_g, T_x, ΔT_x, crystallization behavior and magnetic properties was examined for the alloy series of $Fe_{56}Co_7Ni_7Zr_{10-x}Nb_xB_{20}$ ($x=0$ to 10 at%). The results obtained are summarized as follows.

(1) The glass transition and subsequent supercooled liquid region were observed in the temperature range before crystallization for all the alloys. The T_g and T_x are 814 and 887 K, respectively, for the 0 at%Nb alloy, increase by the dissolution of Nb and show maximum values of 828 and 912 K, respectively, for the alloys containing 2 to 4 at%Nb. The degree of the increase in T_x as a function of Nb content is larger than that for T_g, leading to the maximum ΔT_x of 85 K for the 2 at%Nb alloy. This value is about 20 K larger than the largest value for Fe-based amorphous alloys reported up to date.

(2) The crystallization takes place with a single stage (amorphous $\rightarrow$ α-Fe + γ-Fe + Fe_2Zr + $Fe_{76}Nb_6B_{18}$) for the alloys containing less than about 6 at%Nb, and two stages (amorphous $\rightarrow$ γ-Fe + amorphous $\rightarrow$ γ-Fe + $Co_3Nb_2B_5$ + Ni_8Nb) for the alloys containing more than 8 at%Nb without precipitating Fe_2Zr and Fe_2Nb. The temperature interval of the two exothermic peaks corresponding to the two-stage crystallization is as large as about 150 K. It is to be noticed that the wide supercooled liquid region exceeding 50 K appears even for the alloys with the distinct two-stage crystallization processes.

(3) The I_s, H_c and μ_e at 1 kHz in the optimally annealed state are 0.96 T, 2.0 A/m and 19100, respectively, for the Fe-Co-Ni-Zr-B alloy. However, the I_s and μ_e decrease with increasing Nb content while H_c remains almost unchanged. The resulting I_s, H_c and μ_e are 0.75 T, 1.1 A/m and 25000 for the 2 at%Nb alloy and 0.61 T, 1.1 A/m and 14800 for the 10 at%Nb alloy. Thus, the alloys containing less than about 3 at%Nb exhibit the good combination of the wide supercooled liquid region and good soft magnetic properties. The finding of the new amorphous alloys with the two characteristics is important for the future development of bulk amorphous alloys in the application of soft magnetic materials.

Acknowledgment

The authors are grateful to the Grant-in-Aid for Specially Promoted Research of The Ministry of Education, Science, Sports and Culture for support of this research.

REFERENCES

(1) A. Inoue, K. Ohtera, K. Kita and T. Masumoto: Jpn. J. Appl. Phys., **27** (1988), L2248.
(2) A. Inoue, M. Kohinata, A. P. Tsai and T. Masumoto: Mater. Trans., JIM, **30** (1989), 378.
(3) A. Inoue, T. Zhang and T. Masumoto: Mater. Trans., JIM, **30** (1989), 965.
(4) A. Inoue, H. Yamaguchi, T. Zhang and T. Masumoto: Mater. Trans., JIM, **31** (1990), 104.
(5) A. Inoue, T. Zhang and T. Masumoto: Mater. Trans., JIM, **31** (1990), 177.
(6) T. Zhang, A. Inoue and T. Masumoto: Mater. Trans., JIM, **32** (1991), 1005.
(7) A. Inoue, A. Kato, T. Zhang, S. G. Kim and T. Masumoto: Mater. Trans., JIM, **32** (1991), 609.

(8) A. Inoue and T. Masumoto: Mater. Sci. Eng., **A173** (1993), 1.
(9) A. Inoue, K. Kita, T. Zhang and T. Masumoto: Mater. Trans., JIM, **30** (1989), 722.
(10) A. Inoue, T. Zhang and T. Masumoto: Mater. Trans., JIM, **31** (1990), 425.
(11) A. Inoue, T. Zhang, N. Nishiyama, K. Ohba and T. Masumoto: Mater. Trans., JIM, **34** (1993), 1234.
(12) A. Inoue, T. Saito, H. Yamamoto and T. Masumoto: J. Mater. Sci. Lett., **12** (1993), 946.
(13) A. Peker and W. L. Johnson: Appl. Phys. Lett., **63** (1993), 2342.
(14) A. Inoue, T. Zhamg and T. Masumoto: J. Non-Crsyt. Solids, **156–158** (1993), 473.
(15) A. Inoue: Mater. Trans., JIM, **36** (1995), 866.
(16) A. Inoue: *Nanostructured and Non-Crystalline Materials*, ed. by M. Vazquez and A. Hernando, World Scientific, Singapore (1995), p. 15.
(17) A. Inoue: *Advanced Materials and Processing*, ed. by K. S. Shin, J. K. Yoon and S. J. Kim, The Korean Inst. Metals and Materials, Seoul, (1995), p. 1849.
(18) A. Inoue: Mater. Sci. Forum, **179–181** (1995), 691.
(19) A. Inoue: Sci. Rep. Res. Inst. Tohoku Univ., **A42** (1996), 1.
(20) A. Inoue, Y. Shinohara and J. S. Gook: Mater. Trans., JIM, **36** (1995), 1427.
(21) A. Inoue, A. Takeuchi, T. Zhang and A. Murakami: IEEE Trans. Mag., **32** (1996), 4866.
(22) A. Inoue, T. Zhang, W. Zhang and A. Takeuchi: Mater. Trans., JIM, **37** (1996), 99.
(23) A. Inoue, T. Zhang, A. Takeuchi and W. Zhang: Mater. Trans., JIM, **37** (1996), 636.
(24) A. Inoue, T. Zhang and A. Takeuchi: Mater. Trans., JIM, **37** (1996), 1731.
(25) A. Inoue, T. Zhang and A. Takeuchi: IEEE Trans. Magn., in press.
(26) M. Kikuchi, H. Fujimori, T. Obi and T. Masumoto: Jpn. J. Appl. Phys., **14** (1975), 1077.
(27) C. H. Smith: *Rapidly Solidified Alloys*, ed. by H. H. Liebermann, Marcel Dekker, New York (1993), p. 617.
(28) A. Inoue, T. Zhang, T. Itoi and A. Takeuchi: Mater. Trans., JIM, **38** (1997), 358.
(29) F. R. de Boer, R. Boom, W. C. M. Mattens, A. R. Miedema and A. K. Niessen: *Cohesion in Metals*, Elsevier Science Publishers B.V., Amsterdam (1988).
(30) A. Inoue and J. S. Gook: Mater. Trans., JIM, **36** (1995), 1180.
(31) *Metals Databook*, ed. by Japan Inst. Metals, Maruzen, Tokyo (1983), p. 8.